Quarterly Journal of the
Royal Meteorological Society

The 11-year Solar Cycle Signature in the Southern Hemispheric Winter and its QBO Modulated Effects on the Southern Annular Mode

Journal:	*Quarterly Journal of the Royal Meteorological Society*
Manuscript ID:	QJ-09-0139
Wiley - Manuscript type:	Research Article
Date Submitted by the Author:	03-Jul-2009
Complete List of Authors:	Lu, Hua; British Antactic Survey Gray, Lesley; Reading University, NCAS-Climate, Meteorology Dept. Jarvis, Martin; British Antarctic Survey Baldwin, Mark; Northwest Research Associates, -; Northwest Research Associates, -
Keywords:	Southern Hemisphere, the 11 year solar cycle, Southern Annular Mode, stratosphere troposphere coupling

The 11-year Solar Cycle Signature in the Southern Hemispheric Winter and its QBO Modulated Effects on the Southern Annular Mode

Hua Lu[1,a], Lesley J. Gray[2], Martin J. Jarvis[1], Mark P. Baldwin[3]

Prepared for **Quarterly Journal of the Royal Meteorological Society**

[a] Corresponding author.

[1] H. Lu and M. J. Jarvis, British Antarctic Survey, High Cross, Madingley Road, Cambridge CB3 0ET, England, UK. (email: hlu@bas.ac.uk; mjja@bas.ac.uk)

[2] L. J. Gray, NCAS-Climate, Meteorology Dept., Reading University, Earley Gate, PO Box 243, Reading RG6 6BB, UK. (email: lesley@met.rdg.ac.uk)

[3] M. P. Baldwin, Northwest Research Associates, 4118, 148th Ave, Redmond, WA 98052, USA. (email: mark@nwra.com)

Abstract: This paper updates observations of the 11-year solar cycle (11-yr SC) induced responses in temperature and wind in the Southern Hemisphere (SH) stratosphere and troposphere. In the stratosphere, significant positive solar signals are found in low-latitude stratospheric temperature from May to October. The associated solar signature in zonal wind is characterized by poleward and downward movement of a strengthened subtropical jet and a weakened polar jet. Those stratospheric responses are found to be independent of the equatorial Quasi-biennial Oscillation (QBO) but substantially weakened if the 2002 winter is included. The stratospheric solar signals differ from the Northern Hemispheric (NH) SC responses reported in previous studies and suggest that the stratospheric response to the 11-yr SC depends on the background winter flow regime. In the troposphere, on the other hand, the response to the 11-yr SC is marked by a perturbation of the Southern Annular Mode (SAM) that is modulated by the QBO. In June and July, the SAM is positively correlated with the solar irradiance input when the QBO at 50 hPa is easterly. In August and September, the opposite holds when the QBO is westerly. These tropospheric solar signals are consistent with the known QBO-SC relationship during the NH polar winter and likely to be associated with dynamic processes. Overall, the results reveal some noticeable hemispheric contrasts as well as remarkable similarities in terms of atmospheric responses to the 11-yr SC, aiding further understanding of radiative and dynamical origins of solar forcing in the stratosphere and troposphere.

1. Introduction

There is an increasing body of evidence suggesting that changes associated with the 11-year solar cycle (SC) have detectable effects on the atmospheric circulation (Gleisner and Thejll 2003; Haigh 2003; Coughlin and Tung 2004; Hood,2004; Salby and Callaghan 2006; Lu *et al.* 2007; van Loon *et al.* 2007). It has been found that the 11-yr SC signature in stratospheric temperature is characterized by positive correlations at low latitudes with a vertical double-peaked structure, one in the lower stratosphere and another in the upper stratosphere (Crooks and Gray 2005; Keckhut *et al.* 2005; Claud *et al.* 2008). Absorption of solar ultra violet (UV) radiation by stratospheric ozone causes temperature changes in the regions near the stratopause and this is regarded as the primary cause for the observed solar responses in the upper stratosphere (Haigh 2003; Hood 2004; Gray et al. 2009). In winter, these relatively weak changes may alter the upward propagating planetary-scale waves, and lead to an indirect feedback on the lower stratosphere through a modulation of the stratospheric polar vortex as well as through a weakening of the Brewer-Dobson (BD) circulation (Kodera and Kuroda 2002). The solar effect in zonal-mean zonal wind in the upper stratosphere is marked by a strengthening of the subtropical jet and a poleward and downward movement of westerly anomalies (Kuroda and Kodera 2002; Kodera *et al.* 2003; Gray *et al.* 2004; Matthes *et al.* 2004).

In the late winter of the Northern Hemispheric (NH), Labitzke (1987) and Labitzke and van Loon (1988) observed a more complicated, nonlinear interaction between the Quasi-biennial Oscillation (QBO) in the equatorial lower stratosphere and the 11-yr SC. They found that the polar lower stratospheric temperature is positively correlated with the 11-yr SC when the QBO is westerly (wQBO), and negatively correlated when the QBO is easterly (eQBO; see also Gray *et al.* 2004; Labitzke 2006). By using daily data from European Centre for Medium Range Weather Forecasting (ECMWF) extending from 1958 to 2006, Lu *et al.* (2009) confirmed that the NH 11-yr SC signature in zonal mean temperature and zonal wind can only be detected statistically when the data are grouped according to the phase of the QBO in the equatorial stratosphere. In addition, they also confirmed that the QBO-modulated solar signals move poleward and downward in late winter, suggesting a modulation of sudden stratospheric warmings (SSWs). During solar maximum years, the solar signals tend to descend faster and deeper into the troposphere under wQBO than under eQBO. In particular, the solar signals extend from the upper stratosphere to the surface under wQBO. They found that solar signals in stratospheric temperature were stronger and more robust under wQBO than under eQBO.

Significant responses in the troposphere to the 11-yr SC have also been reported (van Loon and Labitzke 1998; Gleisner and Thejll 2003; van Loon and Meehl 2008). The solar signature in tropospheric temperature is marked by positive correlations at mid-latitudes (van Loon and Labitzke 1998; Crooks and Gray 2005; Lu *et al.* 2007). In the zonal-mean zonal wind, a weakening of the winter upper-tropospheric sub-tropical jet, together with a poleward shift of the mid-latitude jets in both hemispheres appears to be associated with high solar activity (Haigh *et al.* 2005). Idealised model simulations have suggested that the solar influence on the upper troposphere may be due to a modulation of synoptic scale wave activity (Haigh and Blackburn 2006; Simpson *et al.* 2009). It has also been suggested that the influence of the 11-yr SC in the tropical troposphere may be through a suppression of convective activity in the equatorial region resulting from a change in the temperature structure near the tropopause, which is due to a solar-induced change in the BD circulation (Kodera 2004; Matthes *et al.* 2006). In addition, an air–sea feedback mechanism has been proposed to explain the observed tropospheric solar signals (Meehl *et al.* 2003; van Loon *et al.* 2004; Meehl *et al.* 2008). Such a feedback, which is enhanced by a redistribution of the clouds, can also cause dynamic alterations in the troposphere. The tropospheric solar responses associated with this latter process are marked by stronger upward and downward motions in the winter and summer hemispheric subtropics, respectively, during solar maximum years (van Loon *et al.* 2004).

It has also been reported that the 11-yr SC may influence the troposphere through a modulation of the large-scale modes at polar latitudes such as the Northern or Southern Annular Mode (NAM or SAM). The SAM is the leading mode of temporal variability of atmospheric circulation in the Southern Hemisphere (SH) and accounts for ~33% of the total variance of the daily zonally averaged zonal wind in the troposphere (Thompson and Solomon 2002; Marshall 2003). It has been found that the 11-yr SC modulates the spatial structure of the SAM from October through to December (Kuroda and Kodera 2005). In solar maximum years, the solar influence on the SAM extends vertically from the surface to the upper stratosphere while it is capped within the troposphere during solar minimum years. A similar effect was also found for the NAM in the NH winter (Kodera 2002, 2003; Kodera and Kuroda 2005).

Due to the limited data record before the satellite era (*i.e.* pre- September 1978) in the SH and the lack of variability of the SH polar vortex, considerably fewer observational studies on the atmospheric responses to the 11-yr SC have been undertaken for the SH winter than for the NH winter. Due to weaker planetary wave forcing, the SH polar vortex is generally stronger and longer-lived than its NH counterpart. The dynamically more stable condition of the SH winter implies that radiative interaction is likely to play a larger role in the SH winter than in the NH winter, which in turn may result in different atmospheric responses to the 11-yr SC in the SH winter to those observed in the NH winter. Although the solar signals in the SH have been found to be different to those in the NH (Labitzke 2002), little process-based explanation has been provided. An intriguing feature of the 11-yr SC signature in temperature during the SH winter is that the signals appear to be stronger in the equatorial lower stratosphere under eQBO and are mostly confined in the troposphere under wQBO (Labitzke 2002, 2005; Lu *et al.* 2007). As most previous studies used monthly or yearly averages, there is a lack of temporal and spatial detail regarding where those solar signals originate and whether or not the temperature responses are related to changes in the upper stratosphere and how the QBO modulation takes place.

This study complements the recent study of Lu *et al.* (2009) by investigating how the zonal-mean state in the stratosphere and troposphere may respond to the 11-yr SC variability during the SH winter and spring. Daily atmospheric data from January 1979 to December 2006 are used to provide a detailed picture of the solar signal progression from May to October in the SH. The primary objectives are: 1) to examine the intra-seasonal life cycle of the SH 11-yr SC signals in both the stratosphere and the troposphere, *i.e.* when and where the solar signals are initialized, strengthened and weakened; 2) to study the modulating effects of the QBO in both the stratosphere and troposphere; and 3) to identify the radiative or dynamic origin of the detected solar signals. In the context of those primary objectives, we also investigate a possible modulation of the 11-yr SC on the SAM.

2. Data and Methods

Similar to Lu *et al.* (2009), 10.7-cm solar radio fluxes (in units of $10^{-22}Wm^{-2}Hz^{-1}$) are used as a proxy for the 11-yr SC. Daily observed 10.7-cm solar radio fluxes were obtained from the National Geophysical Data Center (NGDC) website (www.ngdc.noaa.gov/stp). To be consistent to Lu *et al.* (2009), 6-month averaged 10.7-cm solar radio fluxes (F_s hereafter), were used in the analysis, where the 6-month period immediately precedes the day when the atmospheric variable averages were taken. Qualitatively similar results can be obtained if the average window of F_s is in the range of 1-6 months.

Observational and modeling studies have shown that the response of the tropospheric circulation to solar changes depends on the precise distribution of the stratospheric perturbations, which may change on monthly or even sub-monthly time-scales (Kodera 2004; Haigh and Blackburn 2006; Matthes *et al.* 2006). To examine the seasonal progression of the solar signals in detail, the atmospheric data used are daily mean zonal winds and temperatures from the ECMWF ERA-40 Reanalysis (September 1957 to August 2002) and ECMWF Operational analyses (September 2002 to December 2006). The ERA-40 dataset has a horizontal resolution of 1.125º in both latitude and longitude on 23 pressure levels from 1000 hPa to 1 hPa (Uppala *et al.* 2005). The Operational data has the same horizontal resolution but only on 21 pressure levels, which are identical to the ERA-40 except without the 600 and 775 hPa levels. For simplicity, only the data for those 21 pressure levels are used here. Both ERA-40 and Operational datasets extend to 1 hPa (~50 km), thus allowing an examination of the solar signals throughout the stratosphere. The daily data have not previously been used for this purpose and this work is therefore complementary to earlier analyses by providing more detailed temporal information of the solar signals in the SH winter and spring. Due to poorly constrained model output, the scarcity of SH radiosonde measurements results in unreliable estimations in ERA-40 before the satellite era. Thus, only data from January 1979 onwards were used.

Nevertheless, weaker but qualitatively similar results are obtainable below 10 hPa if data since 1958 are used.

The QBO was defined using the deseasonalized zonal wind from the blended ERA-40 and Operational data at 0.56°N, 50 hPa. Baldwin and Gray (2005) and Pascoe *et al.* (2005) found that the ERA-40 dataset accurately describes the tropical stratosphere up to ~3 hPa. The phase of the QBO was determined for each specific period after an averaging window of 31-days was applied to both the QBO and the atmospheric variable it correlates to. Transition periods when the absolute values of the QBO were smaller than 2 m s^{-1} were excluded from the analysis. For the monthly correlations, the Free University of Berlin (FUB) QBO index at 50 hPa is also used at various points to confirm results obtained with the ERA-40 derived QBO.

Two SAM indices are used to test the robustness of the correlations. The first is the daily SAM index derived as the leading empirical orthogonal function (EOF) of daily zonal-mean zonal wind over 20°–90°S, from the ECMWF ERA-40 reanalysis for the period of 1958-2006. The details about the method can be found in Baldwin and Thompson (2009). It is found that the SAM index correlates well with that derived from NCEP reanalysis, with correlation coefficient greater than 0.9 in the troposphere and greater than 0.95 in the stratosphere. The second type of SAM index is the station-based index, which extends back to 1957 (Marshall 2003). It was estimated as a monthly mean difference between the mean sea level pressure anomaly at six stations close to 40°S and six stations close to 65°S. For simplicity, these two types of SAM index are referred to hereinafter as ECMWF-SAM and Marshall-SAM, respectively.

Unlike its NH counterpart, stratospheric sudden warmings (SSWs) have hardly ever occurred in the SH winter. Only one major SSW event has occurred during the period under investigation; this was in September, 2002. It has been revealed that the wind and temperature in 2002 appear to be anomalous in a different way to the other years in general and also to those years affected by major volcanic eruptions (Scaife *et al.* 2005). In this study, the dynamic features of 2002 will be briefly discussed in the context of atmospheric response to solar forcing. Possible contamination by the temporary warming of volcanic aerosols has also been examined by comparing results after excluding and including two years of data following three major eruptions (*i.e.* Agung in March 1963, El Chichón in March 1982, and Pinatubo in June 1991). We found that including data affected by major volcanic eruptions results in larger solar signals in the lower stratospheric temperature but has negligible effects in the upper stratosphere. In order to gain a comprehensive understanding of the general behaviour of the 11-yr SC signature in the SH, the two years after each volcanic eruption are excluded from the spatially distributed analyses but included when the temporal evolution of atmospheric variables is displayed.

The main diagnostic tools employed are linear correlation and composite analysis. The statistical confidence levels of the correlations are calculated using the standard Student t-test. The same Monte Carlo significance test used by Lu *et al.* (2007) is used to test the statistical significance of the composite differences.

3. Results

3.1 Solar signature in Temperature

Figure 1 shows the zonal mean temperature (T_{clim}) for May to October (1st column) and temperature differences ΔT_{HS-LS} between high solar (HS) and low solar (LS) conditions (2nd column), all displayed in meridional-height cross section with latitude extending from 30°N to 90°S. During the winter months when the temperature of the SH polar lower stratosphere cools to below 190 K, notably enhanced positive values of ΔT_{HS-LS} are found in the equatorial and subtropical stratosphere. The temperature differences are marked by a vertical-double-maximum structure with ΔT_{HS-LS} up to 3 K at ~5 hPa and 1 K at ~70 hPa in the upper and lower stratospheres, respectively, while minimum, non-significant positive values of ΔT_{HS-LS} are found at ~20-30 hPa. Simultaneously, negative significant ΔT_{HS-LS} are found at mid-latitudes (~50-60°S) at various pressure levels. Near the pole, ΔT_{HS-LS} displays a vertically alternating negative and positive wave-like pattern in late autumn and winter (May-Aug), and then becomes pre-dominantly positive in spring (Sep-Oct). This disturbance pattern at the poles should be ignored because the ERA-40 and Operational temperature analysis over Antarctica is prone to spurious oscillations arising caused by a modeling error; a spurious increase in temperature tends to occur in the upper stratosphere and propagates downwards during winter (Simmons *et al.* 2007). Despite this, the overall pattern of ΔT_{HS-LS} in the stratosphere indicates an increase in the meridional temperature gradient from the equator to mid-latitudes under HS during SH winter. In the troposphere, small regions of temperature increase of ~0.5K is observed at ~30-40°S in September and October and a temperature decrease of ~0.5K is obtained poleward of ~50° from May to September. No significant tropospheric temperature differences are seen at low latitudes.

[[Insert Figure 1 here]]

Time series of the daily temperatures in the upper and lower stratosphere for all the individual years (*i.e.* 1979-2006) are shown in figures 2 and 3, respectively, at a few selected heights and latitudes where maximum confidence levels of the composite differences were found. In figure 2, daily averaged temperature at the equator, 5-10 hPa (top row), at 15°S, 3-7 hPa (mid- row), and at 50°S, 2-5 hPa (bottom row) are compared for HS (1st column) and LS (2nd column) conditions.

[[Insert Figure 2 here]]

[[Insert Figure 3 here]]

Figure 2 shows that, in the upper stratosphere, considerable temperature variations exist for all three selected latitudes and the variation is larger for HS years than for LS years. The larger temperature variation under HS may be partially due to the fact that the variations in high energy UV flux are generally greater for solar maximum than for solar minimum (Lean *et al.* 1997), and partially due to the contaminating effects of the major volcanic eruptions (shown as the blue lines). This increased variability in HS years in mid-winter is especially evident at 45°S, even if the winter of 2002 (shown in purple) is excluded. The 3rd column of figure 2, displays the mean daily temperatures under HS (red) and under LS (grey) conditions. The shaded regions represent 95% confidence intervals for the mean. When the shaded regions do not overlap, it indicates that, during that period, the average temperature differences between the HS and LS groups are significant at or above the 95% confidence level. The unusually active 2002 winter and the volcanic years have been excluded from the HS group to demonstrate that they are not the prime cause of any differences between HS and LS. Statistically significant increased temperatures are evident in HS compared with LS years at the equator and subtropics and lower temperatures are evident at high latitudes. Similar temperature differences can be obtained at other latitudes in the upper stratospheric equatorial and subtropical regions and the pattern and differences are particularly robust during mid-winter. Significant (at a 95% confidence level) temperature differences are found in June and July in the equator/subtropics and in July and August near 50°S, implying that the lower latitude signals lead the higher latitude signals.

Figure 3 shows the corresponding temperature time series for the lower stratosphere at the equator, 15°S, and 55°S and all averaged over 50-70 hPa. It shows that higher temperatures existed for the volcanic eruption affected years near the equator and subtropics, due to the warming effect of the volcanic aerosols. In the 2002 winter, substantially lower temperatures are found in the subtropics accompanied by higher temperatures at 55°S, consistent with anomalously stronger planetary wave activity found in 2002 (Hio and Yoden 2005). However, little significant HS-LS temperature difference is found at the equator although the temperatures are shown to be generally higher at HS than at LS. However, significant positive temperature differences are found in the subtropics from mid-May to mid-September, while negative temperature differences are found in the extratropical lower stratosphere in August and September. Those temperature differences are statistically significant at a 95% confidence level only when 2002 data are excluded, while including volcanic eruption affected years enhances the temperature differences. The fact that a significant temperature difference is found near 15°S but not at the equator may be due to the contaminating effect of the QBO near the tropics (Smith and Matthes 2008). Note that the temperature variability in the subtropics is evidently smaller than at the equator.

The positive temperature differences between HS and LS in the lower stratosphere near the equator and subtropics confirm previous studies and are consistent with a generally weakened BD circulation in solar maximum years with higher temperatures in low latitude lower stratosphere. Gray *et al.* (2009) have demonstrated that the direct effects of irradiance changes in the lower stratosphere are likely to be extremely small and hence cannot account for the observed temperature changes. The lower stratospheric signal is most likely to be of dynamical origin, either directly through a modification of the Brewer-Dobson circulation or indirectly, through changes in ozone transport.

It has been previously reported that, in July and August, the 11-yr SC signals in the equatorial lower stratospheric temperature were statistically weaker when the QBO at 50 hPa is in its westerly phase (wQBO) and stronger when it is in its easterly phase (eQBO) (Labitzke 2005), and the same relationship was observed for the NH winter (Lu *et al*. 2009) and at annual timescale (Lu *et al*. 2007). Figures 1-3 suggests that, in the SH winter, the 11-yr SC signals can be obtained without separating the data according to the phases of the QBO. Additional analysis using linear correlations between 6-month averaged 10.7-cm solar flux F_s and June to September mean temperatures separated into eQBO and wQBO years (not shown) reveal similar spatial patterns of solar signals to those shown in figure 1, and were obtainable as long as the 2002 winter is excluded. However, no significant solar signals can be obtained for the wQBO phase when the 2002 data are included.

The contamination effect of the 2002 data may be due to the fact that in the SH the winter polar vortex is cold, stable and hence pre-dominantly radiatively-driven, while the unprecedented major SSW which occurred in September 2002 made it much more disturbed, due to anomalously stronger planetary wave forcing (Hio and Yoden 2005). The SH 2002 major SSW shared many similarities to the more commonly occurring major warmings in the NH winter and is characterized by a noticeably earlier decrease of the upper stratospheric subtropical jet, and rapid poleward and downward movement of stratospheric wind anomalies (Krüger *et al.* 2005).

Comparing the solar signals obtained in this study to those in the NH winter, the 11-yr SC signatures in the stratosphere are noticeably different. In the NH winter, the 11-yr SC signals in the stratosphere are characterized by strong QBO-modulated solar signals in the high latitudes (Lu *et al.* 2009). The 11-yr SC signals in the SH winter stratosphere are characterized by weak or no signals near the pole. The positive temperature response in the low latitude lower stratosphere suggests a weakened BD circulation at solar maximum. However during the NH winters and the 2002 SH winter, there is an additional complication due to the presence of stronger planetary wave activity that also depends on the phase of the QBO. These planetary waves may give rise to SSWs, which in turn have an opposite effect on the BD circulation and result in an off-setting anomalous cooling effect due to anomalous upwelling near equatorial lower stratosphere.

3.2 Solar Signature in Zonal Wind

Figure 4 is the same as figure 1 except that the temperature is replaced by the zonal-mean zonal wind and the latitude-height cross section is from the equator to 90°S. The climatology of the wind field is characterized by a strengthening and poleward movement of the stratospheric westerly jet from May to July and a gradual weakening and downward movement of the jet thereafter. Shown by the zonal wind differences between HS and LS conditions (ΔU_{HS-LS}), the 11-yr SC signals in stratospheric zonal-mean zonal wind are marked by anomalously strengthened westerlies in the subtropical jet, indicated by positive ΔU_{HS-LS}; this is accompanied by a weakened polar jet, represented by negative ΔU_{HS-LS}, in the upper stratosphere. These westerly and easterly wind anomalies in the upper stratosphere (~1 hPa) appear first in June at ~28°S and ~55°S, respectively. The plots for May indicate that the anomalies may have been generated earlier than June at higher altitude above 1 hPa.

The increase in zonal-mean zonal wind in the upper stratospheric subtropics in HS is consistent with thermal wind balance in the presence of the anomalous latitudinal temperature differences at 3-7 hPa shown in figure 1 (2nd column). Given that the jet maximum is situated at ~60°S, the enhancement of the subtropical side of the jet and weakening of the polar jet signify an equatorward shift of the stratospheric westerly jet at HS. An equatorward shift of the jet suggests a broader and more disturbed vortex at solar maximum, which is consistent with the increased variability of temperature at high solar activity seen in figures 2 and 3. From June to August, those wind anomalies intensify as the winter progresses and as the stratospheric westerly jet moves poleward and downward. The speed of the movement is approximately 5° poleward and ~10 km downward per month. By August, the pair of anomalies descends to the lower stratosphere. With a stable polar vortex, the 11-yr SC signature is characterized by a consistent strengthening of the subtropical jet and weakening of polar jet across the entire winter and early spring. In general, the overall structure of ΔU_{HS-LS} in the stratosphere agrees well with that reported by Kodera and Kuroda (2002).

[[Insert Figure 4 here]]

In the troposphere, the climatology of the zonal-mean zonal wind is characterized by a gradual strengthening of the subtropical jet in the months leading up to July / August (Figure 4, left panel). Zonal wind differences ΔU_{HS-LS} are found primarily in May/June and September. In June, the latitudinal pattern of ΔU_{HS-LS} suggests a weakening of the subtropical jet, a strengthening of the westerlies at 50-70°S with more easterly anomalies at poleward of 70°S. In September, the latitudinal banded structure of ΔU_{HS-LS} is narrower with more easterly anomalies near the tropics, strengthened westerlies at 35-50°S and easterly anomalies at 55-65°S. It will become clearer later in section 3.2, that unlike the stratospheric signals, the tropospheric solar signals are QBO phase dependent.

Figure 5 shows the temporal evolution and variation of the zonal wind in the upper stratosphere for HS and LS conditions, similar to the temperature plots in figures 2 and 3. Daily time series of zonal-mean zonal winds (U) are shown at 35°S averaged over 1-5 hPa (upper panels), and at 65°S averaged over 2-7 hPa (lower panels), for individual years under HS (1st column) and LS (2nd column) conditions are plotted. Lower pressure levels are selected for the 65°S winds as the winds at 1 hPa are less reliable. In general agreement with Kodera and Kuroda (2002), it shows that the seasonal progression of the subtropical and polar jets can be characterized by three temporal stages: 1) a monotonic increase of the strength of the subtropical jet from March to June, during which small variability is associated with U; 2) a decrease of the strength of the subtropical jet from July to August and a simultaneous increase of the polar jet with noticeably larger variability in U, likely due to vertically propagating planetary waves from the lower stratosphere mid-latitudes; 3) a rapid decrease of the polar jet after September towards the end of winter. Generally, the same temporal progression pattern holds for both HS and LS conditions, and for a range of latitudes, *i.e.* 28-40°S for the winds near the subtropical jet and 60-70°S for the winds near the polar jets, respectively.

[[Insert Figure 5 here]]

Significant differences between HS and LS conditions are found for both subtropical and polar winds in the upper stratosphere, as demonstrated by the daily mean values of U under HS (red line) and under LS (grey line) in the 3rd column of figure 5. Note that 2002 data and the years contaminated by the major volcanic eruptions are excluded. Under HS, the subtropical winds peak in late-June/early-July with maximum speeds of 80-100 m s^{-1}, while at LS, the subtropical winds peak in June with maximum speeds of 65-85 m s^{-1}. Significant differences in the subtropical winds between HS and LS are found from mid-June to late August, when the variability of U is the largest. For the polar jet, noticeable wind differences between HS and LS conditions are found primarily at a later time (*i.e.* from mid- June to mid- July). Once again, the polar wind differences appear to lag the subtropical differences by about 15-days to one month.

A sensitivity analysis, in which the diagnostics were repeated with different years excluded, indicates that including the data affected by the major volcanic eruptions and the major SSW tends to reduce the statistical confidence levels; the most significant effect comes from the 2002 data (shown in purple). In 2002, the subtropical jet started to decelerate in mid-May, much earlier than in any other year. For the polar jet, however, the zonal-mean zonal wind in June and July 2002 was noticeably stronger than average but became weaker than average in August and September. The abnormal behaviour of the zonal wind in 2002 is similar to that in the NH when a major SSW occurs, and likely results from anomalously strong planetary waves from the lower atmosphere (Hio and Yoden 2005; Krüger *et al.* 2005).

3.3 The QBO Modulated Tropospheric Signature

Figure 6 shows the temporal evolution of the solar signals in zonal-mean zonal winds by showing the running correlations between F_s and 31-day averaged zonal-mean zonal wind for a series of latitudes at 25°S, 30°S, 35°S, 40°S, and 45°S (from top to bottom). The data have been separated into wQBO years (1st column) and eQBO years (2nd column). The correlations are plotted at the 16th-day of the 31-day averages. Again, the years affected by volcanic eruptions and 2002 data are excluded from the analysis. A clear downward and poleward descent of positive solar signals from the upper stratosphere to the lower stratosphere can be seen for both QBO phases. At all latitudes this response commences early under wQBO (beginning March) and later under eQBO (beginning of June). Another marked difference is that the solar signals extend much deeper under wQBO, reaching down to the surface, especially at 35-45°S during late winter and spring, which is coincident with the period of maximum planetary wave amplitudes (Thompson and Solomon 2002).

[[Insert Figure 6 here]]

There are other noteworthy correlation features in figure 6. For both QBO phases, negative correlations tend to both precede and follow the positive signals in the mid-latitude stratosphere, although once again, these extend deeper into the troposphere in wQBO years. The main summertime signal in the troposphere extends from December to March and is strongest at 25-35°S, possibly linked to the previously observed weakening and poleward shift of the mid-latitude jets (Haigh 2003; Crooks and Gray 2005) which has been modeled using a simple GCM (Haigh *et al.* 2005; Haigh and Blackburn 2006; Simpson *et al.* 2009).

Returning to the mid-winter signal, figure 7 shows the correlation between 6-month averaged 10.7-cm solar flux F_s and zonal-mean zonal wind (U) averaged for June and July (top panels) and August and September (bottom panels), under wQBO (left-hand panels), and eQBO (right-hand panels). Data for 2002 and the years affected by major volcanic eruptions are excluded. In June and July, positive solar signals appear at 15-40°S in the upper stratosphere and extend to 10 hPa while negative signals appear at 50-70°S in both phases of the QBO. In August and September, the paired positive and negative solar signals move poleward and downward.

[[Insert Figure 7 here]]

However, in wQBO years the signal is relatively coherent throughout the depth of the atmosphere and shows a deep latitudinally banded correlation structure extending into the troposphere especially in August-September. In contrast, the eQBO years show a tropospheric anomaly in June/July, of the opposite sign. The structure in June-July under eQBO is marked by negative correlations in the subtropical lower stratosphere/upper troposphere (~20°S, 100-200 hPa), positive correlations at 50-

70°S, 100-1000 hPa and negative correlations at 75-85°S, 300-100 hPa. They suggest a weakening of the tropospheric westerly jet with polarward migration of zonal wind anomalies under solar maximum conditions. This correlation pattern is similar to that which resulted from the simple GCM simulations of Haigh *et al.* (2005) with anomalous heating assigned near the equatorial lower stratosphere. According to Haigh and Blackburn (2006) and Simpson *et al.* (2009), such a response in terms of zonal-wind acceleration and deceleration in different tropospheric regions is associated with dynamical adjustments of zonally-asymmetric synoptic wave forcing in response to changes in stratospheric heating at solar maxima.

In August-September, the tropospheric solar signals in zonal winds under wQBO phase are characterized by a band of positive correlation at ~30-40°S and a band of negative correlation at ~50-60°S, both of which extend from the surface to the stratosphere up to 10 hPa. The correlation pattern associated with wQBO in August-September implies an equatorward shift of the westerly jet. In general, these tropospheric correlation patterns are consistent with the composite differences shown in figure 4. It suggests that the early winter solar signal in June in figure 4 is dominated by the signals coming from eQBO phase years while the late winter solar signal in September is dominated by the signals coming from wQBO phase years. In addition, it is clearly evident that the solar signals in the upper stratosphere tend to be out of the phase to those in the troposphere under eQBO while the solar signals in the stratosphere and troposphere are in phase under wQBO, consistent with that shown in figure 6.

3.4 Solar Signal in the Sothern Annular Mode

It is known that the changes in zonal-mean zonal wind in the tropospheric westerly jet during the SH winter are primarily affected by changes in wave forcing (Lorenz and Hartmann 2001) and the effects are projected onto the large scale atmospheric mode, *i.e.* the Southern Annular Mode (SAM) (Thompson *et al.* 2005). Figure 8 shows the running correlations between F_s and a linearly detrended 31-day averaged ECMWF-SAM under wQBO (left-hand panels), eQBO (right-hand panels), for 1979-2006 (top panels), and 1968-2006 (bottom panels). Slightly weaker but qualitatively similar correlations can be obtained for 1958-2006 period. The correlations are once more plotted at the 16th-day of the 31-day averages of the SAM and the 2002 winter and the years affected by the major volcanic eruptions are excluded. In the stratosphere and for both QBO phases, positive solar signals first appear at 1 hPa in early winter (~June) and descend to 10 hPa by August. The correlation coefficients and statistical confidence levels are slightly lower under wQBO than under eQBO, possible indicating stronger wave disturbances under HS/wQBO. Despite this, the general patterns confirm that the solar signals in the stratosphere are largely QBO phase independent. In the troposphere, under wQBO, significant negative correlations are found in August to September while positive correlations are detected in May and June. Under eQBO, significant positive correlations are found in June to July. Similar correlation patterns are found when data from pre-satellite era are included, as exemplified in the 2nd column of figure 8, which results from using 1968-2006 data. The statistically significant positive solar signals in the SAM under eQBO in early winter exist for ~30-40 days while the negative correlations under wQBO in late winter and spring last ~50-60 days.

[[Insert Figure 8 here]]

Further tests were carried out by performing the same analysis but replacing the ECMWF-SAM by the SAM indices derived from NCEP reanalysis. Almost identical correlation patterns were obtained except for the positive correlations in the upper troposphere to the lower stratosphere in May and June under wQBO. In those regions, no significant correlations were detected in May and June when NCEP-SAM was used, suggesting that the correlations below 10 hPa in May and June are not statistically robust.

[[Insert Figure 9 here]]

To further test the robustness of the solar signals in the SAM, scatter plots of 6-month averaged F_s versus the station-based monthly Marshall-SAM are shown in figure 9. Figure 9(a) shows that there is a significant negative correlation (r = -0.51, $p < 0.03$) between March-August mean F_s and the August-September averaged SAM under wQBO. This implies that, under wQBO, the 11-yr SC accounts for ~25% of the variance in the August-September mean SAM. Figure 9(b) shows that there is a significant positive correlation (r = -0.71, p < 0.01) between January-June mean F_s and the June-July averaged SAM under eQBO. This implies that, under eQBO, the 11-yr SC may account for up to 50% of the variance in the June-July SAM.

4. Conclusion and Discussions

In this study, we have found statistically significant 11-yr SC signals in the SH stratosphere and troposphere during the winter and spring. In general, there are significant 11-yr SC signals in both the stratosphere and troposphere. The signals in the stratosphere are QBO phase independent, unlike in the NH winter (Lu *et al*. 2009). In the troposphere, on the other hand, the solar signal appears to be associated with dynamic processes that are modulated by the QBO.

In the stratosphere in early winter (May, June), significant positive 11-yr SC temperature anomalies are found in HS years compared with LS years, over the latitude range between 30°N and 30°S, while negative signals occur in the 40-60°S latitude range (figure 1). The signals suggest a solar induced latitudinal temperature gradient from the equator to mid-latitudes. The enhanced temperature gradient causes a strengthening of subtropical zonal winds in the upper stratosphere through thermal wind balance (figure 4). In general, these stratospheric solar signals appear to be consistent with a radiatively-driven response and are in good agreement with previous studies (Kodera and Kuroda 2002; Matthes *et al.* 2004).

In mid and late SH winter, the solar signature in zonal-mean zonal wind is characterized by a poleward and downward movement of an anomalously strengthened subtropical jet and weakened polar jet in HS years (figure 4). This mid-winter development of the solar signals appears to be a dynamical response, since the direct radiatively-driven temperature signals in the lower stratosphere are very small (Hood 2004; Gray *et al*. 2009). We note that the poleward movement of the anomalies is much slower than the corresponding poleward progression of the solar signal in the NH winter (Lu *et al*. 2009), consistent with the fact that the SH vortex is less disturbed than its NH counterpart and the zonally-averaged climatological position of the vortex is consistently further equatorward in the SH. The solar signals in figure 4 therefore signify a strengthening of the equatorward part of the stratospheric westerly jet and a weakening of the poleward part under HS conditions. This change of distribution in stratospheric zonal-mean zonal wind can be explained by the presence of more frequent wave disturbances at the edge of the vortex in HS years, so that the maximum westerly winds extend further into the subtropics. It is noteworthy that the most significant solar responses occur in mid-winter, when the variability in the SH stratosphere is the largest. In particular, the larger temperature variability at 45-55°S is found in HS years (figures 2-3), consistent with a more disturbed, weakened polar jet at solar maximum (figure 5).

In summary, the stratospheric solar signature in the more stable SH vortex appears to be an increase in poleward wave disturbances in solar maximum years, and this response is not dependant on the phase of the QBO. In the NH winter, the observations show a more disturbed vortex in HS/wQBO years and LS/eQBO years (Labitzke and van Loon 1988), so the SH solar response resembles the NH response under wQBO conditions, when the background winds in the polar stratosphere is relatively strong and undisturbed (Holton and Tan 1980; Lu *et al*. 2008). This suggests that the stratospheric solar response may be dependent on the background winter flow regime. In a cold, undisturbed winter regime (majority of years in SH; wQBO years in the NH), the stratospheric response to the 11-yr SC is characterized by an increase in wave disturbance. In a warmer, more disturbed winter regime (eQBO years in the NH) there is an increase in wave disturbance under solar minimum conditions. We note that inclusion of the more disturbed SH winter (2002) in our analysis resulted in degraded solar response signals and the temporal evolution of temperature and zonal wind suggest that the 2002 southern winter shares many of the characteristics of the more disturbed winter regime, the typical behavior often found the NH winter during eQBO years.

In the lower atmosphere, we have shown that the 11-yr SC perturbs the tropospheric and surface SAM in the SH winter and spring and that these perturbations depend on the phase of the QBO, in contrast to the stratospheric signals. In June and July, the 11-yr SC signature projects positively onto the SAM under eQBO, implying a poleward shift of the mid-latitude westerly jet at solar maximum. In August and September, it projects negatively onto the SAM under wQBO, implying an equatorward shift of the mid-latitude westerly jet at solar maximum. These results are shown to be robust by using different SAM data sets and for different periods.

This time evolution of the tropospheric response is remarkably similar to the time evolution of the QBO-SC relationship in the NH winter stratosphere, described by Lu *et al*. (2009). Gray *et al*.(2004) noted an additional modulation of the timing of SSWs during NH winter, which were found to occur more often under LS/eQBO in early to mid-winter and under HS/eQBO in mid- to late winter (see also Labitzke 2005; Lu *et al.* 2009). The QBO modulated tropospheric signals shown in figure 7 can also be interpreted as more poleward wave forcing under LS/eQBO in early SH winter and under HS/wQBO in late winter and spring. We therefore find that in the cold, undisturbed winter regime of the SH, the QBO modulation of the 11-yr solar signals is only evident in the troposphere, as either a poleward or equatorward shift of the tropospheric mid-latitude jet. Those tropospheric responses are also reflected by consistent and significant correlations between the SAM and the 11-yr SC (figures 8-9). These new findings provide a physical explanation of the previous results from multiple regression analysis (Haigh and Roscoe 2006), which have shown that neither the NAO nor SAM index are significantly correlated with either the 11-yr SC or the QBO, but they are significantly correlated with a combined SC/QBO index generated by multiplication of the 11-yr SC and the QBO time series.

It remains intriguing that the 11-yr SC projects significantly onto the tropospheric SAM, which is a characteristic of the polar surface circulation, through a QBO modulation. This is particularly puzzling given the fact that the dominant solar signature lies in the upper stratosphere, the QBO is an equatorial phenomenon. In late winter to spring, the positive solar signals in mid-latitude stratospheric zonal-mean zonal wind are shown to connect into the troposphere under wQBO but not under eQBO. Likewise, stronger vertical connection of solar signals was also reported in the NH during late winter and spring under wQBO (Lu *et al.* 2009). This enhanced stratosphere-troposphere coupling in late winter and spring under HS/wQBO requires an explanation and may help to understand the tropospheric SC/QBO signals. One possibility involves vertically propagating planetary waves from the troposphere to the stratosphere and subsequent descent of zonal wind anomalies into the troposphere (Chen and Robinson 1992; Song and Robinson 2004) but the mechanisms are not well understood and it is not clear why this coupling should be most effective in wQBO years. Another possibility involves a tropospheric response to stratospheric heating anomalies (Simpson *et al*. 2009) which may depend on the background climatology of the stratospheric wind field and on the strength of the equatorial lower stratospheric heating anomaly, which is likely to be positive under HS/wQBO conditions. Model simulations are needed to provide a clearer explanation as it is hard to tell from the observational data how and where these tropospheric solar signals originate or whether the dominant mechanism resides primarily in the troposphere or the stratosphere.

Acknowledgements

Acknowledgements: HL and MJJ were supported by the UK Natural Environment Research Council (NERC). LJG was supported by the UK NERC National Centre for Atmospheric Science (NCAS). MPB was funded by NSF under the US CLIVAR program and the Office of Polar Programs.

References

Baldwin MP, Gray LJ. 2005. Tropical stratospheric zonal winds in ECMWF ERA-40 reanalysis, rocketsonde data, and rawinsonde data. *Geophys. Res. Lett.* **32**: L09806, doi:10.1029/2004GL022328.

Baldwin MP, Thompson DWJ. 2009. A critical comparison of stratosphere-troposphere coupling indices. *Q. J. R. Meteorol. Soc.* (in press).

Chen P, Robinson WA. 1992. Propagation of planetary waves between the troposphere and stratosphere. *J. Atmos. Sci.* **49**: 2533–2545.

Claud C, Cagnazzo C, Keckhut P. 2008. The effect of the 11-year solar cycle on the temperature in the lower stratosphere. *J. Atmos. Sol.-Terr. Phys.* **70**: 2031–2040.

Coughlin KT, Tung KK. 2004. 11-year solar cycle in the stratosphere extracted by the empirical mode decomposition method, in *Solar Variability and Climate Change*, edited, pp. 323-329, PERGAMON-ELSEVIER SCIENCE LTD, Killington.

Crooks SA, Gray LJ. 2005. Characterization of the 11-year solar signal using a multiple regression analysis of the ERA-40 dataset. *J. Clim.* **18**: 996-1015.

Gleisner H, Thejll P. 2003. Patterns of tropospheric response to solar variability. *Geophys. Res. Lett.* **30**: L1711, doi:1710.1029/2003GL017129.

Gray LJ, Crooks SA, Pascoe CA, Sparrow S, Palmer M. 2004. Solar and QBO influences on the timing of stratospheric sudden warmings. *J. Atmos. Sci.* **61**: 2777-2796.

Gray LJ, Rumbold ST, Shine KP. 2009. Stratospheric temperature and radiative forcing response to the 11-year solar cycle changes in irradiance and ozone. *J. Atmos. Sci.* (in press).

Haigh JD. 2003. The effects of solar variability on the Earth's climate. *Philos. Trans. R. Soc. Lond. Ser. A-Math. Phys. Eng. Sci.* **361**: 95-111.

Haigh JD, Blackburn M, Day R. 2005. The response of tropospheric circulation to perturbations in lower stratospheric temperature. *J. Clim.* **18**: 3672–3691.

Haigh JD, Blackburn M. 2006. Solar influences on dynamical coupling between the stratosphere and troposphere. *Space Sci. Rev.* **125**: 331–344.

Haigh JD, Roscoe HK. 2006 Solar influences on polar modes of variability. *Meteorol. Zeitschrift* **15**: 371-378.

Hio Y, Yoden S. 2005. Interannual variations of the seasonal march in the Southern Hemisphere stratosphere for 1979-2002 and characterization of the unprecedented year 2002. *J. Atmos. Sci.* **62**: 567-580.

Holton JR, Tan HC. 1980. The influence of the equatorial quasi-biennial oscillation on the global circulation at 50 mb. *J. Atmos. Sci*. **37**: 2200-2208.

Hood LL. 2004. Effects of solar UV variability on the stratosphere, in *Solar variability and its effect on the Earth's atmosphere and climate system*, edited by J. Pap *et al.* AGU Monograph Series, Washington D.C.

Keckhut P, Cagnazzo C, Chanin ML, Claud C, Hauchecorne A. 2005. The 11-year solar-cycle effects on temperature in the upper stratosphere and mesosphere Part I: Assessment of observations. *J. Atmos. Sol.-Terr. Phys.* **67**: 940–947.

Kodera K. 2002. Solar cycle modulation of the North Atlantic Oscillation: Implication in the spatial structure of the NAO. *Geophys. Res. Lett.* **29**: L1218, doi:1210.1029/2001GL014557.

Kodera K, Kuroda Y. 2002. Dynamical response to the solar cycle. *J. Geophys. Res.* **107**: D4749, doi:4710.1029/2002JD002224.

Kodera K. 2003. Solar influence on the spatial structure of the NAO during the winter 1900-1999. *Geophys. Res. Lett.* **30**: L1175, doi:1110.1029/2002GL016584.

Kodera K, Matthes K, Shibata K, Langematz U, Kuroda Y. 2003. Solar impact on the lower mesospheric subtropical jet: A comparative study with general circulation model simulations. *Geophys. Res. Lett.* **30**: L1315, doi:10.1029/2002GL016124.

Kodera K. 2004. Solar influence on the Indian Ocean Monsoon through dynamical processes. *Geophys. Res. Lett.* **31**: L24209, doi:10.1029/2004GL020928.

Kodera K, Kuroda Y. 2005. A possible mechanism of solar modulation of the spatial structure of the North Atlantic Oscillation. *J. Geophys. Res.*, **110**: D02111, doi:02110.01029/02004JD005258.

Krüger K, Naujokat B, Labitzke K. 2005. The unusual midwinter warming in the Southern Hemisphere stratosphere 2002: A comparison to Northern Hemisphere phenomena. *J. Atmos. Sci.* **62**: 603-613.

Kuroda Y, Kodera K. 2002. Effect of solar activity on the Polar-night jet oscillation in the northern and southern hemisphere winter. *J. Meteorol. Soc. Jpn.* **80**: 973-984.

Kuroda Y, Kodera K. 2005. Solar cycle modulation of the southern annular mode. *Geophys. Res. Lett.* **32**: L13802, doi:10.1029/2005GL022516.

Labitzke K. 1987. Sunspots, the QBO, and the stratospheric temperature in the north polar-region. *Geophys. Res. Lett.* **14**: 535-537.

Labitzke K, van Loon H. 1988. Associations between the 11-year solar-cycle, the QBO and the atmosphere 1. The troposphere and stratosphere in the Northern Hemisphere in winter. *J. Atmos. Terr. Phys.* **50**: 197-206.

Labitzke K. 2002. The solar signal of the 11-year sunspot cycle in the stratosphere: Differences between the Northern and Southern summers. *J. Meteorol. Soc. Jpn.* **80**: 963-971.

Labitzke K. 2003. The global signal of the 11-year sunspot cycle in the atmosphere: When do we need the QBO? *Meteorol. Zeitschrift* **12**: 209-216.

Labitzke K. 2005. On the solar cycle-QBO relationship: A summary. *J. Atmos. Sol.-Terr. Phys.* **67**: 45-54.

Labitzke K, Kunze M, Bronnimann S. 2006. Sunspots, the QBO and the stratosphere in the North Polar Region - 20 years later. *Meteorol. Zeitschrift* **15**: 355-363.

Lean JL, Rottman GJ, Kyle HL, Woods TN, Hickey JR, Puga LC. 1997. Detection and parameterization of variations in solar mid- and near-ultraviolet radiation (200-400 nm). *J. Geophys. Res.* **102**: 29939-29956.

Lorenz, D. J., D. L. Hartmann 2001. Eddy-zonal flow feedback in the Southern Hemisphere. *J. Atmos. Sci.* **58**: 3312-3327.

Lu H, Jarvis MJ, Graf H-F, Young PC, Horne RB. 2007. Atmospheric temperature response to solar irradiance and geomagnetic activity. *J. Geophys. Res.* **112**: D11109. DOI: 11110.11029/12006JD007864.

Lu H, Baldwin MP, Gray LJ, Jarvis MJ. 2008. Decadal-scale changes in the effect of the QBO on the northern stratospheric polar vortex. *J. Geophys. Res.* **113**: D10114. DOI: 10110.11029/12007JD009647.

Lu H, Gray LJ, Baldwin MP, Jarvis MJ. 2009. Life cycle of the QBO-modulated 11-year solar cycle signals in the Northern Hemispheric winter. *Q. J. R. Meteorol. Soc.*, **135**: 1030-1043.

Marshall GJ. 2003. Trends in the Southern Annular Mode from observations and reanalyses. *J. Clim.* **16**: 4134-4143.

Matthes K, Langematz U, Gray LJ, Kodera K, Labitzke K. 2004. Improved 11-year solar signal in the Freie Universität Berlin Climate Middle Atmosphere Model (FUB-CMAM). *J. Geophys. Res.* **109**: D06101, doi:06110.01029/02003JD004012.

Matthes K, Kuroda Y, Kodera K, Langematz U. 2006. Transfer of the solar signal from the stratosphere to the troposphere: Northern winter. *J. Geophys. Res.* **111**: D06108, doi:06110.01029/02005JD006283.

Meehl GA, Washington WM, Wigley TML, Arblaster JM, Dai A. 2003. Solar and greenhouse gas forcing and climate response in the twentieth century. *J. Clim.* **16**: 426-444.

Meehl GA, Arblaster JM, Branstator G, van Loon H. 2008. A coupled air-sea response mechanism to solar forcing in the pacific region. *J. Clim.* **21**: 2883-2897.

Pascoe CL, Gray LJ, Crooks SA, Juckes MN, Baldwin MP. 2005. The quasi-biennial oscillation: Analysis using ERA-40 data. *J. Geophys. Res.* **110**: D08105, doi:10.1029/2004JD004941.

Salby ML, Callaghan PF. 2006. Relationship of the quasi-biennial oscillation to the stratospheric signature of the solar cycle. *J. Geophys. Res.* **111**: D06110, doi:01029/02005JD006012.

Scaife AA, Jackson DR, Swinbank R, Butchart N, Thornton HE, Keil M, Henderson L. 2005. Stratospheric vacillations and the major warming over Antarctica in 2002. *J. Atmos. Sci.* **62**: 629-639.

Simmons AS, Uppala, D, Kobayashi S. 2007. *ERA-Interim: New ECMWF reanalysis products from 1989 onwards*. Newsletter 110-Winter 2006/07, ECMWF, 11 pp.

Simpson IR, Blackburn M, Haigh JD. 2009. The role of eddies in driving the tropospheric response to stratospheric heating perturbations. *J. Atmos. Sci.* (in press).

Smith AK, Matthes K. 2008. Decadal-scale periodicities in the stratosphere associated with the solar cycle and the QBO. *J. Geophys. Res.* **113**: D05311, doi:05310.01029/02007JD009051.

Song Y, Robinson WA. 2004. Dynamical mechanisms for stratospheric influences on the troposphere. *J. Atmos. Sci.* **61**: 1711–1725.

Thompson DWJ, Solomon S. 2002. Interpretation of recent Southern Hemisphere climate change. *Science* **296**: 895-899.

Thompson DWJ, Baldwin MP, Solomon S. 2005. Stratosphere-troposphere coupling in the Southern Hemisphere. *J. Atmos. Sci.* **62**: 708-715.

Uppala SM *et al*. 2005. The ERA-40 reanalysis. *Q. J. R. Meteorol. Soc.* **131**: 2961-3012.

van Loon H, Labitzke K. 1998. The global range of the stratospheric decadal wave. Part I: Its association with the sunspot cycle in summer and in the annual mean, and with the troposphere. *J. Clim.* **11**: 1529-1537.

van Loon H, Meehl GA, Arblaster JM. 2004. A decadal solar effect in the tropics in July-August. *J. Atmos. Sol.-Terr. Phys.* **66**: 1767-1778.

van Loon H, Meehl GA, Shea DJ. 2007. Coupled air-sea response to solar forcing in the Pacific region during northern winter. *J. Geophys. Res.* **112**: D02108, doi:02110.01029/02006JD007378.

van Loon H, Meehl GA. 2008. The response in the Pacific to the sun's decadal peaks and contrasts to cold events in the Southern Oscillation. *J. Atmos. Sol.-Terr. Phys.* **70**: 1046-1055.

Figure captions

Figure 1. Left: monthly averages of zonal-mean zonal temperature (in units of K) for May to October (top to bottom), displayed as lined contour plots in meridional-height cross section from 30°N to 90°N and from 1000 hPa to 1 hPa. Right: same as the left panels but displayed as coloured contour plots for the composite differences of temperature between high solar and loss solar conditions (HS-LS). The areas enclosed within the grey lines indicate that the differences are statistically significant from zero with a confidence level of 90% or above, calculated using a Monte-Carlo trial based non-parametric test. The years belonging to the group of HS are: 1979-1983, 1989-1992, and 1999-2003 and the years belonging to the group of LS include: 1984-1988, 1994-1998, and 2004-2006. The years affected by the major volcanic eruptions and 2002 are excluded.

Figure 2. Daily averaged zonal-mean temperatures (K) at 0.56°N averaged over the pressure levels from 5 to 10 hPa (1^{st} row), 15°S averaged over the pressure levels from 5 to 10 hPa (2^{nd} row), 50°S averaged over the pressure levels from 3 to 10 hPa (3^{rd} row), for HS (1^{st} column), LS (2^{nd} column) together with daily mean values for HS (the line with red shading) and LS (the line with grey shading) conditions (3^{rd} column). The shaded regions represent the 95% confidence intervals of the mean. In the HS group, the years in which data might be affected by the major volcanic eruptions (*i.e.* 1982, 1983, 1992, and 1993) are shown as blue lines and the 2002 data are shown as the purple line.

Figure 3. As in Figure 2 but for temperatures at 0.56°N, 15°S, and 55°S, all averaged over the pressure levels from 50 to 70 hPa.

Figure 4. As in Figure 1 but the zonal-mean zonal wind in units of m s^{-1}.

Figure 5. As in Figure 2 but for zonal-mean zonal wind (m s^{-1}) at 35°S, 1-5 hPa (1^{st} row), 65°S, 2-7 hPa (2^{nd} row).

Figure 6. Running correlations between F_s and zonal-mean zonal wind at 25°S, 30°S, 35°S, 40°S, and 45°S (top to bottom), under eQBO (1^{st} column) and eQBO (2^{nd} column), displayed in time-height cross section. The QBO, polar temperature and zonal-mean zonal wind are averaged using a 31-day running window and F_s is defined as 6-month averaged values of F10.7-cm solar radio flux proceeding the wind averages. Solid, dashed

and black lines are positive, negative and zero correlations, respectively. Contour interval is ±0.1. The light and dark grey shaded areas indicate that the correlations are statistically significant at confidence levels greater than 90% and 95%, respectively.

Figure 7. Linear correlations between 6-month averaged F10.7-cm solar flux (F_s) and June-July (1st row) and August-September (2nd row) zonal-mean zonal wind under wQBO (1st column) and eQBO (2nd column). The number of data points (*i.e.* years) used to calculate the correlation coefficients (*r*) are indicated on the top of each panel. The use of lines and shadings are the same as for Figure 6.

Figure 8. Running correlation between F_s and linearly de-trended daily ECMWF-SAM under wQBO (left-hand panels) and eQBO (right-hand panels), displayed in time-height cross section and when data from 1979-2006 (top panels), 1968-2006 (bottom panels) are used. A 31-day running window is applied to the SAM. The use of lines and shadings are the same as for Figure 6.

Figure 9. (a) scatter plot of $F_{s\ \mathrm{Mar\text{-}Aug}}$ and August and September mean linearly detrended Marshall-SAM index when the QBO is in its westerly phase. (b) scatter plot of $F_{s\ \mathrm{Jan\text{-}Jun}}$ and June and July mean Marshall-SAM index when the QBO is in its westerly phase. The data are shown in actual years with two-digit numbering, and a solid line shows the linear regression to the data. Note that the QBO has changed its phase from June to September months in 1957, 1958, 1959, 1965, 1966, 1972, 1975, 1980, 1990, 1991, 2003 and 2006. Those years are excluded. The years affected by the major volcanic eruptions and 2002 are also excluded.

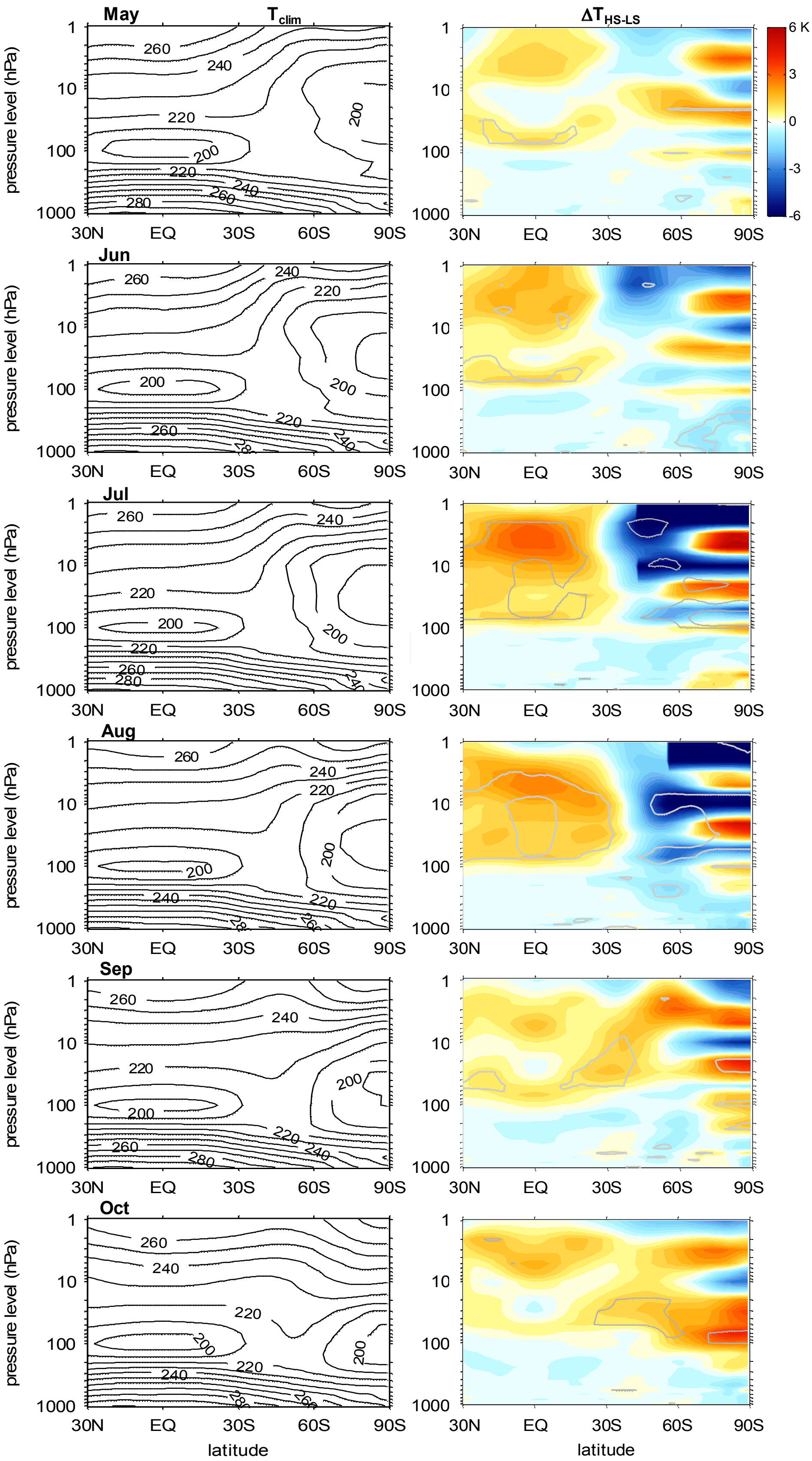
May
Jun
Jul
Aug
Sep
Oct
T_{clim}
ΔT_{HS-LS}
pressure level (hPa)
latitude
30N EQ 30S 60S 90S
6 K
3
0
-3
-6

Figure 1

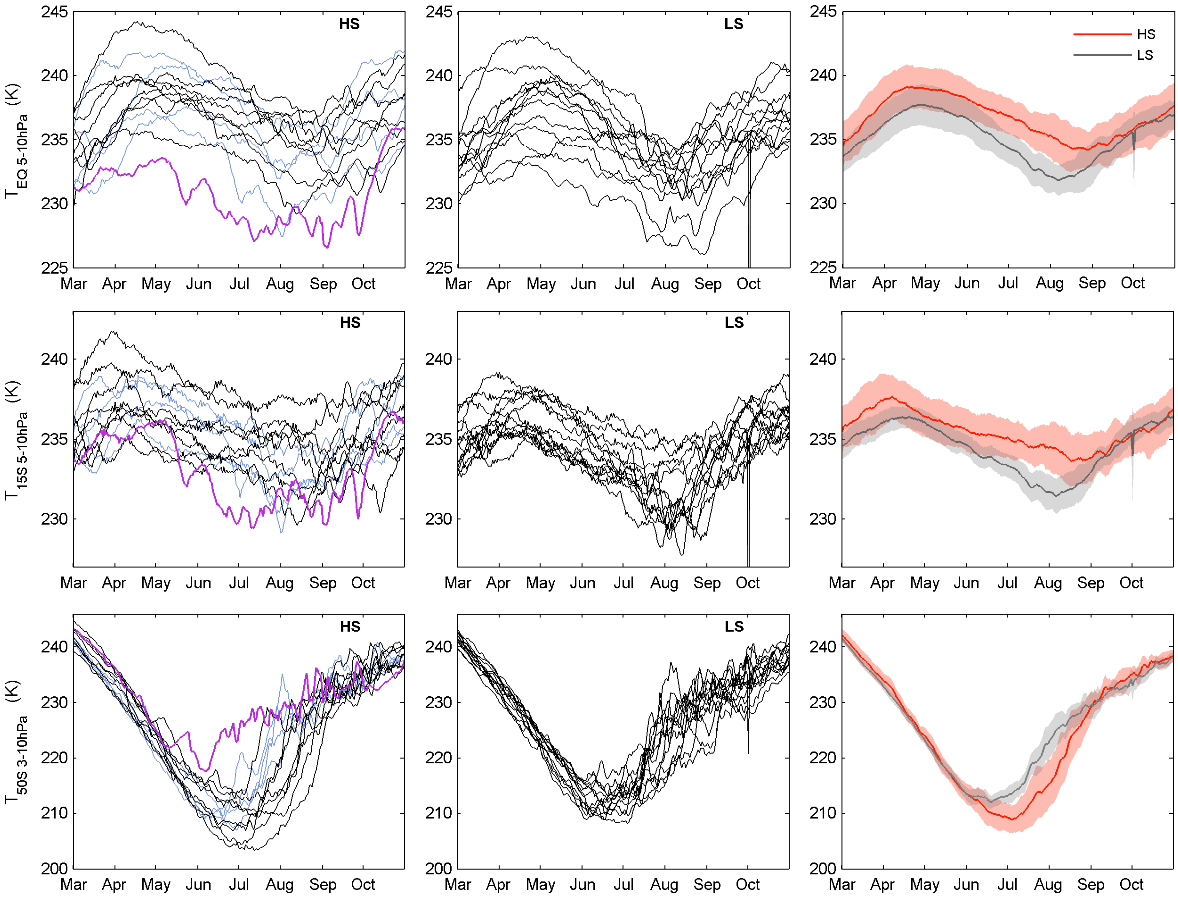
HS
LS
HS
LS
$T_{EQ\ 5\text{-}10hPa}$ (K)
$T_{15S\ 5\text{-}10hPa}$ (K)
$T_{50S\ 3\text{-}10hPa}$ (K)
Mar Apr May Jun Jul Aug Sep Oct

Figure 2

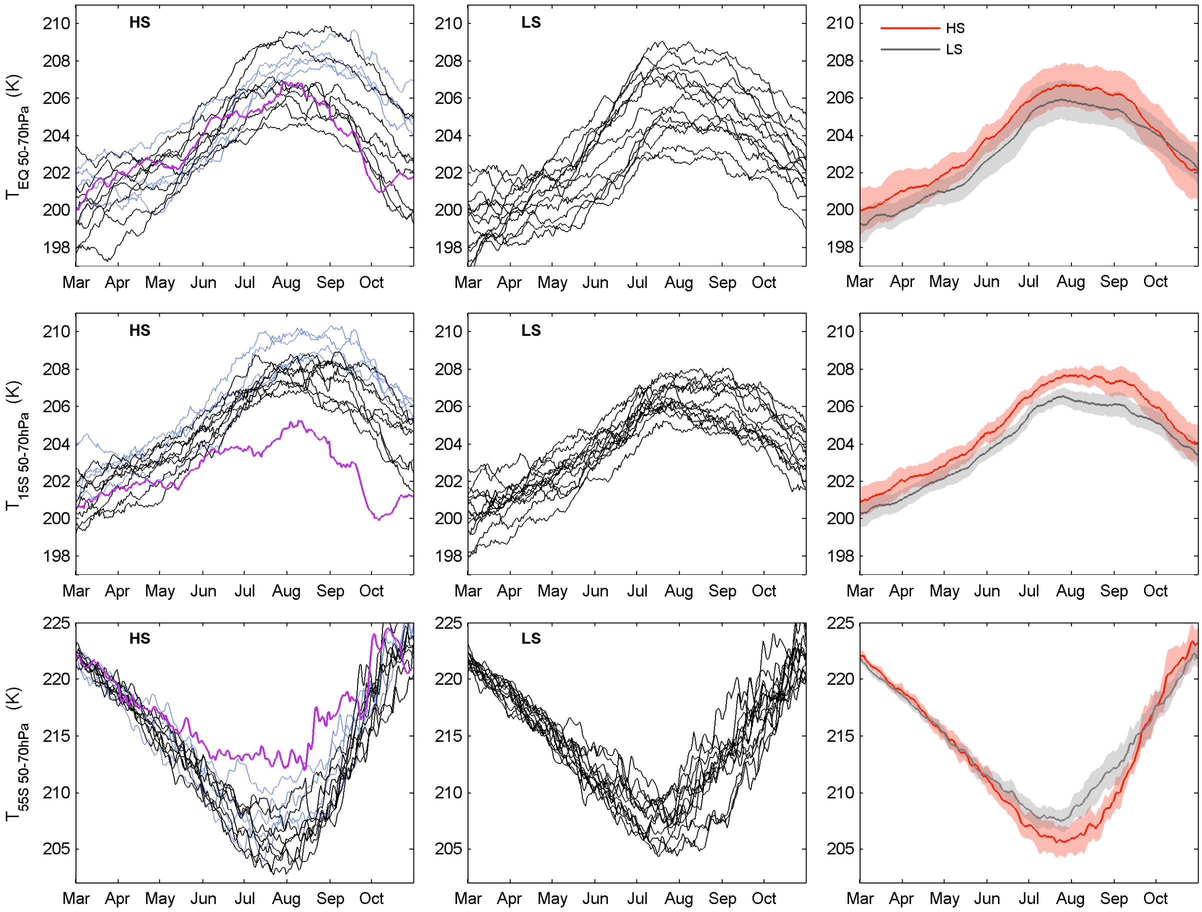
HS
LS
HS
LS
$T_{EQ\ 50\text{-}70hPa}$ (K)
$T_{15S\ 50\text{-}70hPa}$ (K)
$T_{55S\ 50\text{-}70hPa}$ (K)
210
208
206
204
202
200
198
225
220
215
210
205
Mar Apr May Jun Jul Aug Sep Oct

Figure 3

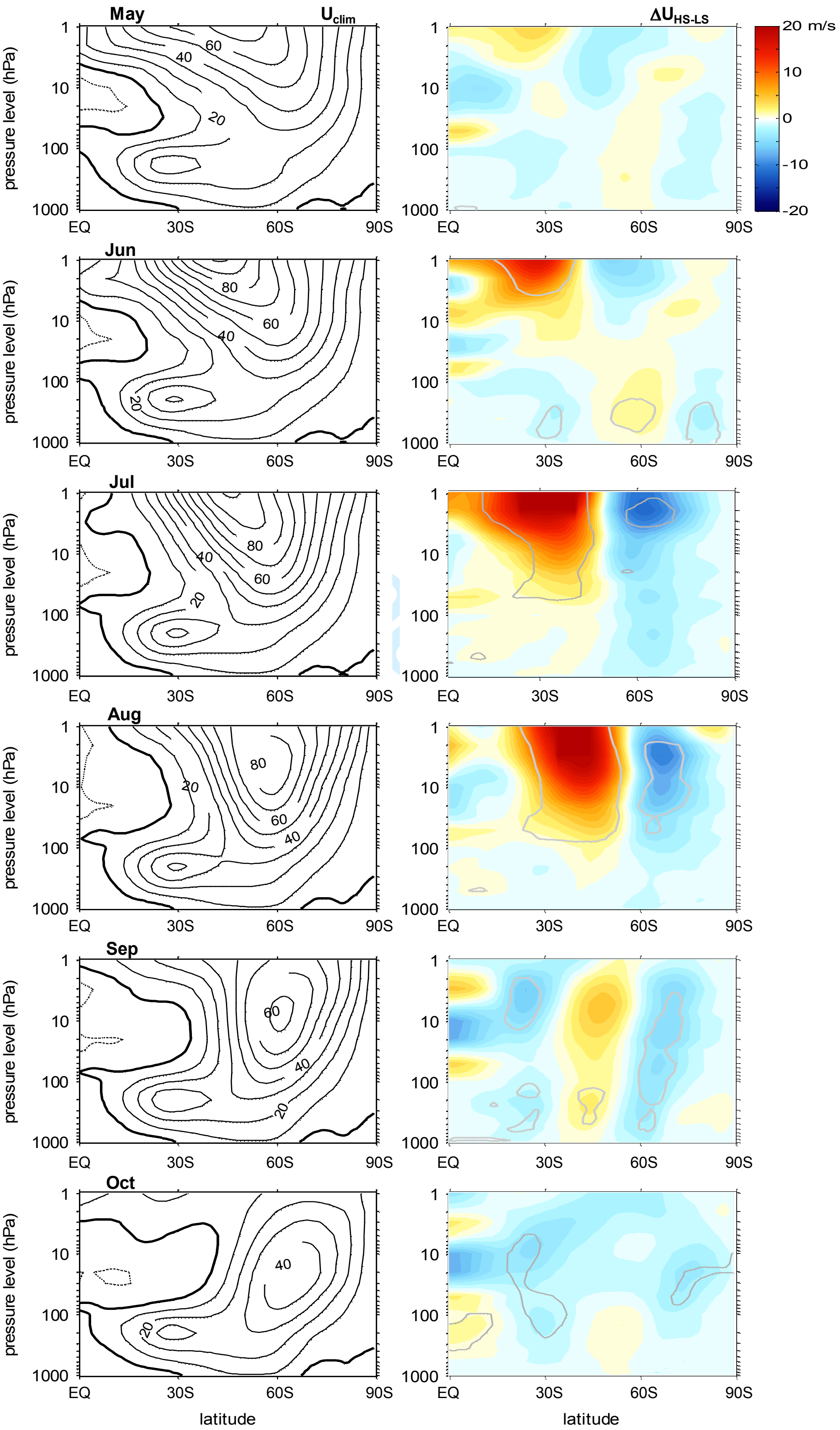
May
U_{clim}
$\Delta U_{HS\text{-}LS}$
20 m/s
10
0
-10
-20
Jun
Jul
Aug
Sep
Oct
pressure level (hPa)
1
10
100
1000
EQ
30S
60S
90S
latitude

Figure 4

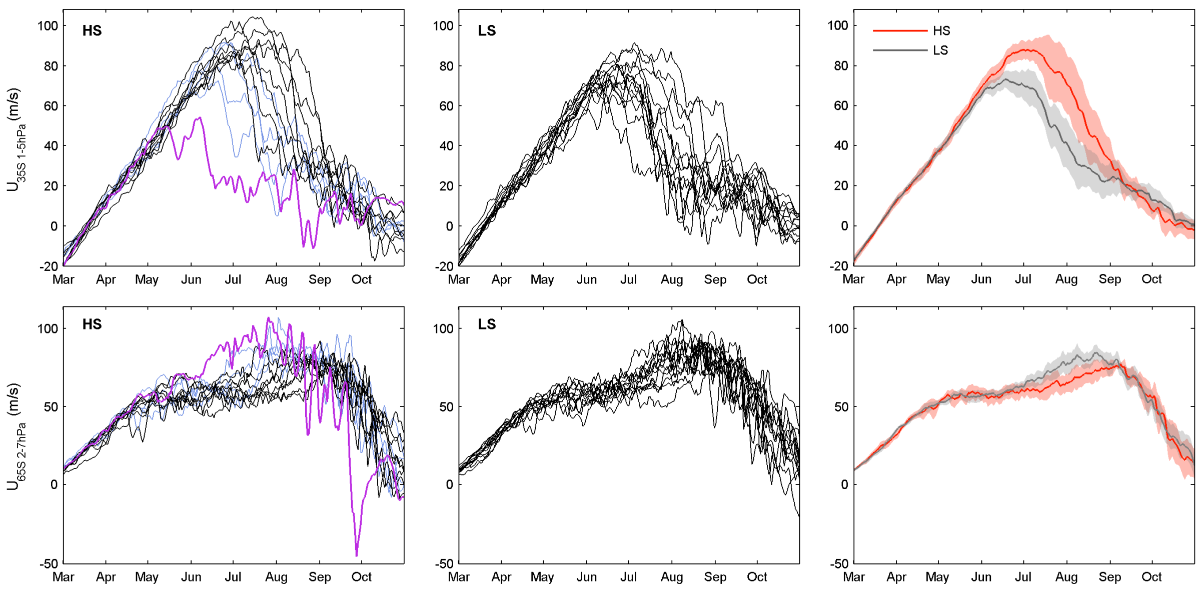
HS
LS
HS
LS
$U_{35S\ 1\text{-}5hPa}$ (m/s)
$U_{65S\ 2\text{-}7hPa}$ (m/s)
Mar
Apr
May
Jun
Jul
Aug
Sep
Oct

Figure 5

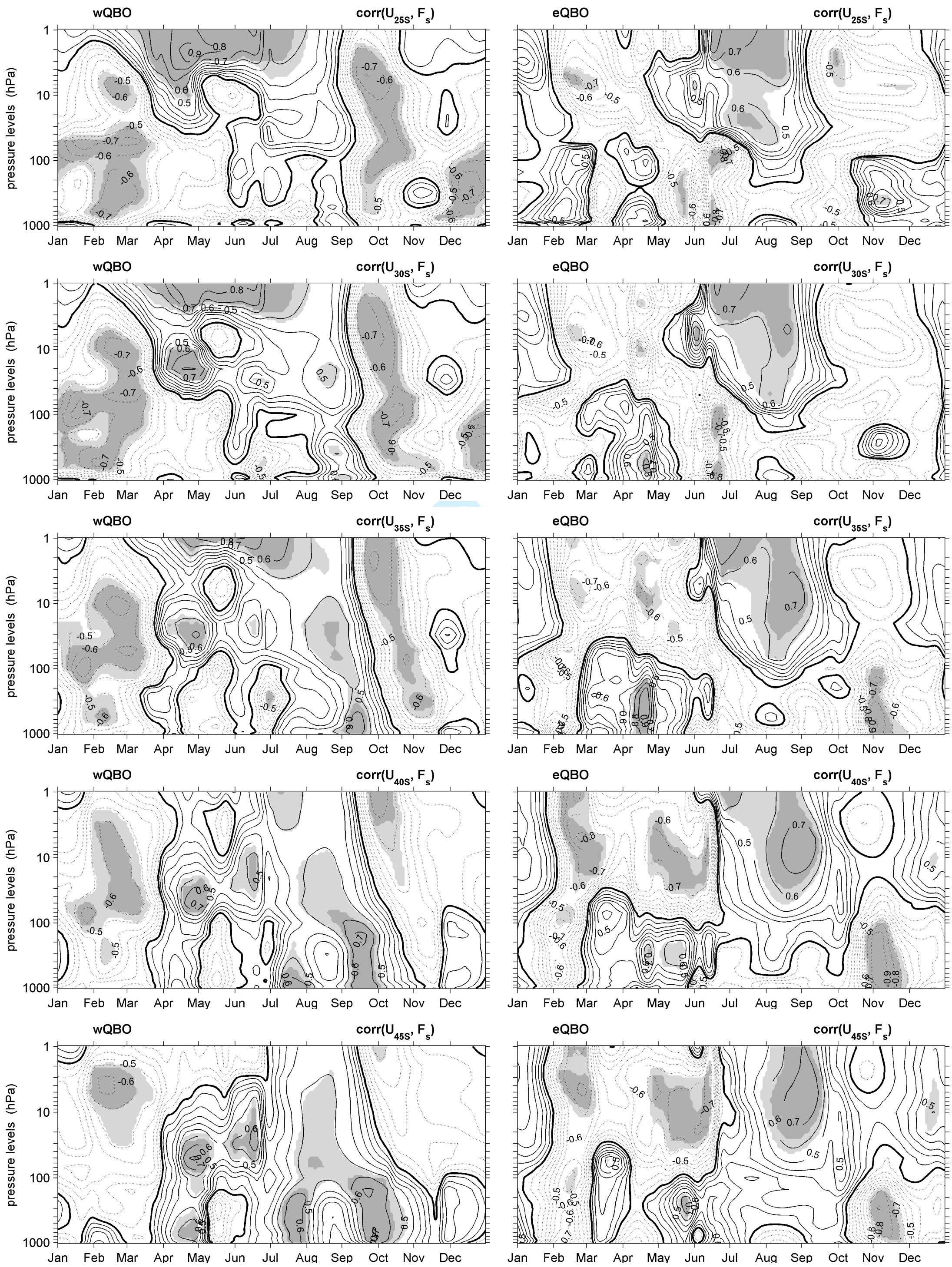
wQBO
corr(U25S', Fs)
eQBO
corr(U25S', Fs)
wQBO
corr(U30S', Fs)
eQBO
corr(U30S', Fs)
wQBO
corr(U35S', Fs)
eQBO
corr(U35S', Fs)
wQBO
corr(U40S', Fs)
eQBO
corr(U40S', Fs)
wQBO
corr(U45S', Fs)
eQBO
corr(U45S', Fs)
pressure levels (hPa)
Jan Feb Mar Apr May Jun Jul Aug Sep Oct Nov Dec

Figure 6

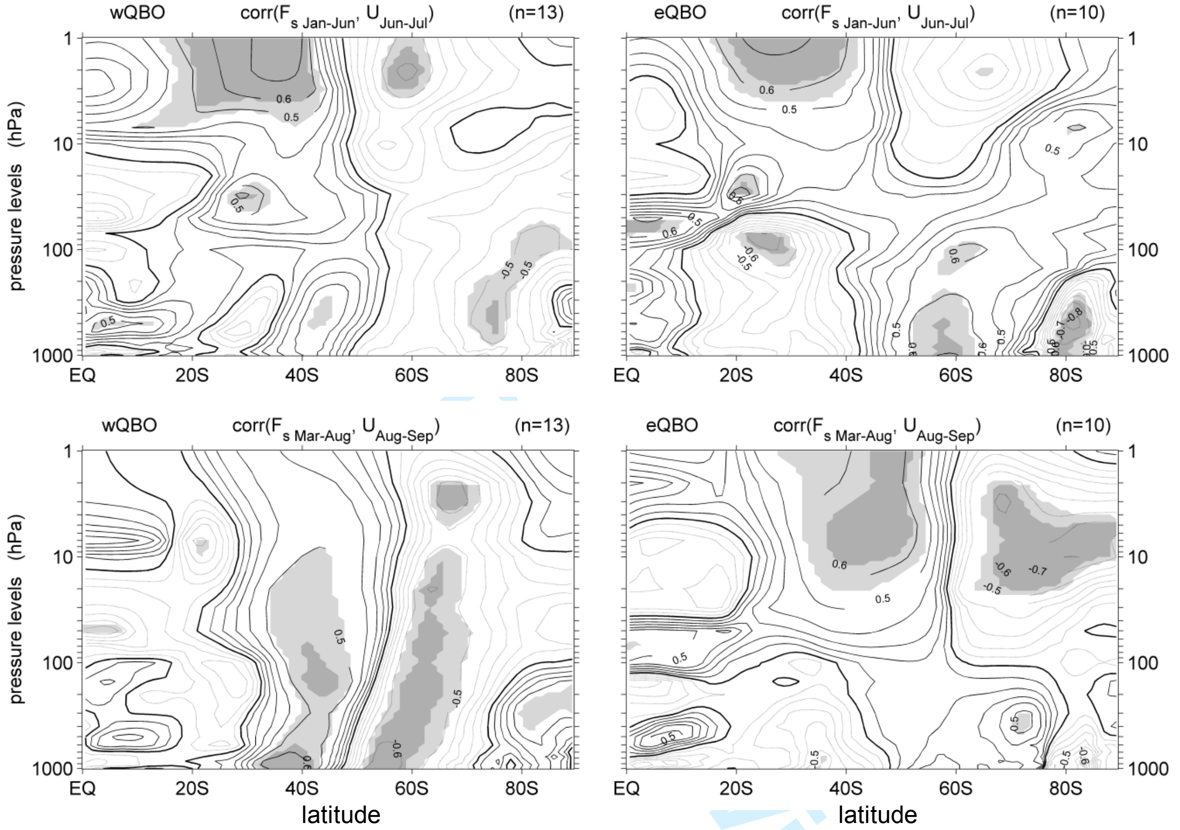

wQBO
corr(F s Jan-Jun, U Jun-Jul)
(n=13)
eQBO
corr(F s Jan-Jun, U Jun-Jul)
(n=10)
wQBO
corr(F s Mar-Aug, U Aug-Sep)
(n=13)
eQBO
corr(F s Mar-Aug, U Aug-Sep)
(n=10)
pressure levels (hPa)
1
10
100
1000
EQ
20S
40S
60S
80S
latitude

Figure 7

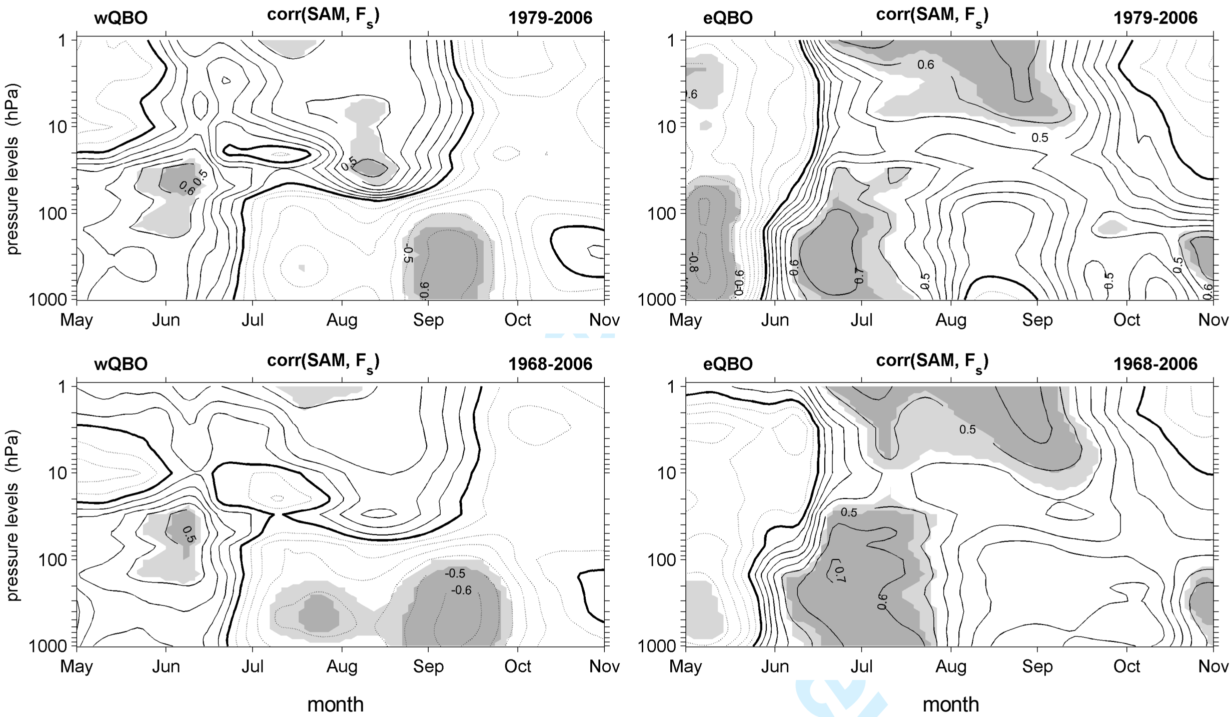
wQBO
corr(SAM, F_s)
1979-2006
eQBO
corr(SAM, F_s)
1979-2006
wQBO
corr(SAM, F_s)
1968-2006
eQBO
corr(SAM, F_s)
1968-2006
pressure levels (hPa)
1
10
100
1000
May
Jun
Jul
Aug
Sep
Oct
Nov
month

Figure 8

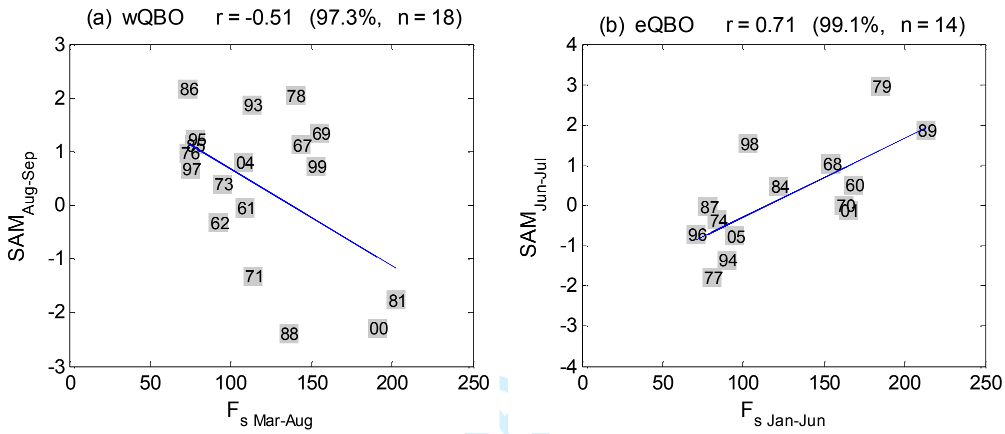
(a) wQBO r = -0.51 (97.3%, n = 18)
SAM Aug-Sep
F s Mar-Aug
86
93
78
95
69
67
76
04
99
97
73
61
62
71
81
88
00
(b) eQBO r = 0.71 (99.1%, n = 14)
SAM Jun-Jul
F s Jan-Jun
79
89
98
68
84
60
87
70
01
74
96
05
94
77

Figure 9